Semicond. Sci. Technol. **11** (1996) 300–307. Printed in the UK

Nonlinear photothermal modulated optical reflectance and photocurrent phenomena in crystalline semiconductors: II. Experimental

Robert E Wagner and Andreas Mandelis

Photothermal and Optoelectronic Diagnostics Laboratory, Department of Mechanical Engineering, University of Toronto, Toronto, Ontario M5S 1A4, Canada

Received 30 August 1995, accepted for publication 14 November 1995

Abstract. Experimental photothermal modulated optical reflectance (PMOR) and photocurrent (PC) data from silicon and germanium samples have been obtained at high laser pump beam intensities and correlated with a theoretical model of nonlinear carrier recombination. In principle, the PMOR signal consists of both thermal and Drude (free-carrier) components; nonlinear recombination influences it through its direct effect on the modulated carrier density, and its indirect effect on the modulated sample temperature. All of the five samples discussed in this work showed evidence of nonlinear carrier recombination in their PC and PMOR behaviour. Although few of the PMOR data were indicative of a dominant Drude component, the effect of nonlinear recombination upon the carrier density was quite apparent in the PC data which were obtained to correlate with the PMOR data. The experimental results clearly indicate that the PMOR effect is sensitive to nonlinear recombination, albeit not to as large a degree as the transverse photocurrent.

1. Introduction

Photothermal modulated optical reflectance (PMOR) in a crystalline material is due to a combined mechanism involving thermal and Drude (free-carrier) modulation effects [1–3]. Theoretically, expressions for the modulated sample temperature, ΔT, and the modulated free-carrier density, ΔN, have been obtained in order to express the PMOR signal as the modulated reflectance, ΔR

$$\Delta R = \frac{\partial R}{\partial T}\Delta T + \frac{\partial R}{\partial N}\Delta N \tag{1}$$

where $\partial R/\partial T$ is the temperature reflectance coefficient and $\partial R/\partial N$ is the Drude reflectance coefficient. ΔN is obtained by solving the carrier diffusion equation, and ΔT is obtained by solving the heat diffusion equation. When the carrier and heat diffusion equations exhibit a significant degree of nonlinear character, primarily with large pump beam powers, the thermal and Drude effects have been modelled in the one-dimensional limit using a finite-difference technique and assuming quadratic and cubic terms besides the conventional linear dependences in the carrier recombination rate equation [4]

$$\frac{\partial N}{\partial t} = D\frac{\partial^2 N}{\partial x^2} - g_1(N - N_0) - g_2(N - N_0)^2 - g_3(N - N_0)^3 + S(x)(1 + e^{i\omega t}). \tag{2}$$

Here, $\Delta N \equiv N - N_0$ represents either the excess free-electron density n, or the excess hole density p, and N_0 is the equilibrium carrier density. D is the average carrier diffusion coefficient for electrons and holes [4]. g_1 is the inverse of the linear carrier lifetime, τ. g_2 is the quadratic carrier recombination coefficient, and is usually associated with band-to-band radiative recombination. g_3 is the Auger (cubic) carrier recombination coefficient. $S(x)f(t)$ is the volume number density of carriers generated per unit time, and $f(t) = 1 + e^{i\omega t}$ is the temporal modulation function of the excitation beam. It has further been estimated that the temperature gradients induced in the sample have little or no influence on carrier transport [4]. If the carrier density is expressed as

$$N(x, t) = N_0 + \sum_{m=1}^{\infty} N_m(x)e^{i\omega(m-1)t} \tag{3}$$

when equation (3) is substituted into equation (2) it is found that each harmonic $e^{i\omega mt}$ is associated with a separate nonlinear differential equation. The finite-difference approach to solving equation (2) reveals that when nonlinear recombination dominates over linear recombination, the fundamental-frequency modulated carrier density at the surface (experimentally accessible by the transverse photocurrent signal [5]) has a sublinear dependence on the excitation intensity. On the contrary,

0268-1242/96/030300+08$19.50

the thermal component of the PMOR signal exhibits a weak supralinear dependence on intensity, whereas the phase lag is much more sensitive to nonlinear recombination. Theoretically, the PC signal contains contributions proportional to the number of photocarriers integrated over the thickness of the sample from both the d.c. carrier density N_1, equation (3), and from the first-harmonic component N_2:

$$\sum N_1 \equiv \sum_{i=1}^{n} N_1(i) \tag{4a}$$

and

$$\sum N_2 \equiv \sum_{i=1}^{n} N_2(i). \tag{4b}$$

Here, n is the number of layers into which the thickness L of the sample has been divided in the finite difference calculation [4].

The effect of nonlinear carrier recombination on the modulated sample temperature, ΔT, in the photoreflectance of equation (1) can be numerically modelled using the finite-difference method with the nonlinear heat diffusion equation [6]:

$$\frac{\partial T}{\partial t} = \beta_s \frac{\partial^2 T}{\partial x^2} + \frac{E_g \beta_s}{k_s}[g_1(N - N_0) + g_2(N - N_0)^2 + g_3(N - N_0)^3] + \frac{(h\nu - E_g)\beta_s I \alpha}{k_s} \exp(-\alpha x)(1 + e^{i\omega t}) \tag{5}$$

where T is the sample temperature, β_s is the sample thermal diffusivity, E_g is the energy gap, k_s is the sample thermal conductivity, $h\nu$ is the pump photon energy and α is the pump absorption coefficient. The first term on the right-hand side of equation (5) contains the free-carrier density N, and represents the heat liberated when the photocarriers recombine non-radiatively. The second term, which is proportional to $h\nu - E_g$, represents the heat released to the sample following intraband thermalization of the hot photocarriers after they are generated by absorption of the pump photons.

2. Experimental and discussion

2.1. Photocurrent behaviour

Transverse, first-harmonic a.c. photocurrent versus intensity data have been obtained from various industrial Ge and Si samples, all of which showed nonlinear effects at high enough laser pump-beam intensities. The PC signal is an important diagnostic because it *directly* probes the free-carrier density, albeit in a contacting manner, and is thus indicative of whether or not nonlinear recombination should be significant during PMOR experiments which employ similar or greater excitation levels. The experimental arrangement for transverse PC measurements, figure 1, resulted in a transverse electric field which was not uniform with depth into the sample. In fact, the electrical contacts were made on the front surface of the sample, rather than on the side edges, so the magnitude of the electric field was largest at the surface and decreased with depth. This

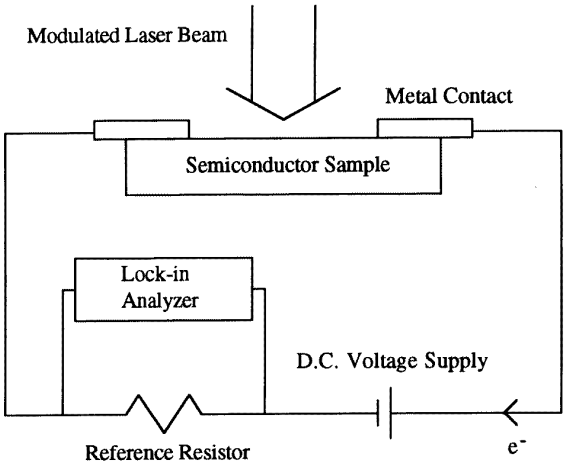

Figure 1. Schematic diagram of experimental apparatus used for measuring the transverse modulated photocurrent.

contact geometry and the visible-range wavelength of the carrier photoexciting radiation tended to sample the carrier density much more at the surface than in the bulk, because the electric field was largest at the surface, and the optical absorption coefficient for both Ge and Si wafers was very high at 514.5 nm. Therefore, it was assumed that the transverse a.c. photocurrent measurements were providing an indication of $N_2(1)$, rather than ΣN_2, where $n = 1$ represents the surface layer of thickness $\Delta x = L/n$.

Modulated transverse PC data were obtained for five different samples (table 1), using a beam-intensity modulation frequency of 1 kHz (unless otherwise noted), and a spot-size diameter of 1 to 2 mm, so as to remain within the one-dimensional (1D) signal regime, in agreement with the theoretical model [4]. Figure 2, curve (a), depicts data obtained for the sample of crystalline germanium (c-Ge). For this material, at lower powers the PC was a linear function of the pump intensity ($I^{0.94}$), but the data became sublinear as the intensity was increased. The high-power intensity dependence ($I^{0.32}$) correlates well with the type of behaviour expected when Auger recombination is dominant and diffusion is negligible [4]. This good correlation is somewhat surprising, since the optical absorption length in the c-Ge was [7] about 0.167 μm, which is much less than the carrier diffusion length; therefore, carrier diffusion must have been important for the c-Ge. The model of [4] clearly indicates that for strong surface generation, one expects $N_2(1) \propto I^{0.48}$ and $\Sigma N_2 \propto I^{0.06}$. Since the observed PC intensity dependence for the c-Ge was intermediate between these two extremes ($\sim I^{0.32}$), *it appears that a mixture of surface and bulk behaviour was present, and that the surface contribution dominated the bulk effect.*

Figure 2, curve (b), shows transverse, first-harmonic PC data obtained for the c-Si1 sample. For low excitation levels the PC increased linearly with I, but transition to a sublinear power law ($I^{0.63}$) occurred as the intensity was raised. Due to the short optical absorption length in this sample [8] at 514.5 nm, diffusion effects were likely to be important. In terms of the theoretical model [4], figure 2(a),

Table 1. Description of various germanium and silicon samples.

Sample	Description	Resistivity (Ω cm)
c-Ge	⟨111⟩, Ga-doped, p-type	15
c-Si1	⟨100⟩, n-type	100
c-Si2	⟨100⟩, bulk: c-Si1 properties; surface layer; As-doped by ion implantation	100 (surface) 100 (bulk)
c-Si3	⟨100⟩, p-type	2.3
c-Si4	⟨100⟩, n-type	65

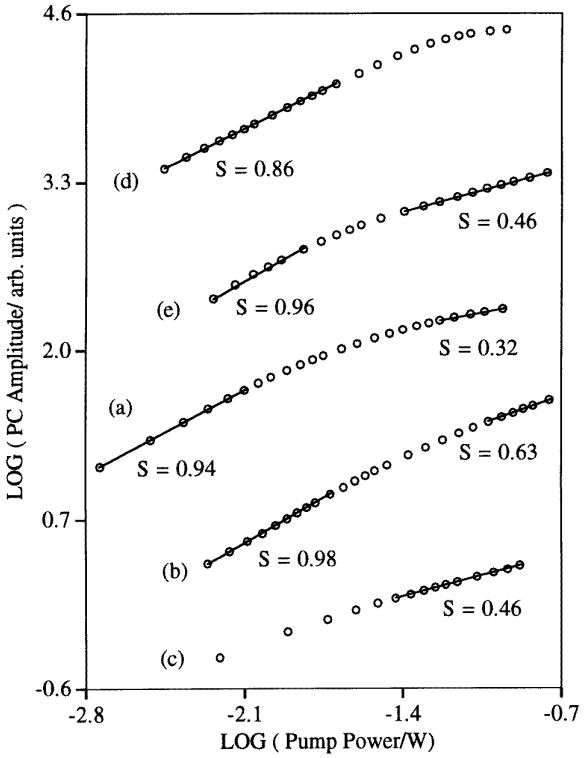

Figure 2. Modulated PC amplitude (arbitrary units) versus absorbed pump power (W). The excitation wavelength is 514.5 nm and f = 1 kHz. The various samples are: (*a*) c-Ge; (*b*) c-Si1; (*c*) c-Si2, 10 kHz; (*d*) c-Si3; and (*e*) c-Si4 (see table 1). The slopes of the linear sections are represented by the quantity S.

the two-thirds power law is theoretically predicted for $N_2(1)$ when quadratic recombination is present and when carrier generation giving rise to strong diffusion effects is localized near the front surface.

Figure 2, curve (c), displays the intensity dependence of the PC for the c-Si2 material. At the higher power levels the PC showed an $I^{0.46}$ behaviour, which is theoretically predicted for $N_2(1)$ in [4], figure 4(*a*), when Auger recombination is dominant, and diffusion is significant (surface-localized carrier generation). Since the c-Si2 sample had a doped, low-resistivity surface layer, it is very reasonable to assume that *most of the PC was due to a thin layer of material near the surface, and that bulk effects were negligible*.

Figure 2, curve (d), shows PC data obtained for the c-Si3 sample when the excitation power was varied. At low powers the PC increased as $I^{0.86}$, which does not correlate with any of the theoretical predictions [4]. At the highest intensities, the power-law exponent showed a tendency to decrease below 0.86. It appears that carrier recombination in the c-Si3 sample is not well described by any of the terms in equation (2). This may have been either due to a nonlinear surface recombination effect with a complicated dependence upon the carrier density or the result of intracarrier system interactions owing to the large free-carrier densities of this low-resistivity sample.

Table 2. Summary of recombination behaviour for various germanium and silicon samples obtained from photocurrent data.

Sample	PC(I) behaviour	Recombination mode
c-Ge	$I^{0.94} \rightarrow I^{0.32}$	Linear → Auger (?)
c-Si1	$I^{0.98} \rightarrow I^{0.63}$	Linear → quadratic
c-Si2	$I^{0.46}$	Linear (?) → Auger
c-Si3	$I^{0.86} \rightarrow$ saturation	Surface effect (?)
c-Si4	$I^{0.96} \rightarrow I^{0.46}$	Linear → Auger

Finally, figure 2, curve (e), depicts PC(I) data for the c-Si4 material. This sample exhibited a clear transition from linear behaviour at low intensities, to a power law ($I^{0.46}$) at higher excitation levels. Judging from the excellent correlation of this data with [4], figure 4(a), it appears that *Auger recombination was dominant for the c-Si4 sample at the higher intensities;* also, as expected, diffusion effects appear to be significant.

A summary of the PC(I) behaviour depicted in figure 2 is given in table 2, which also provides information regarding plausible recombination mechanisms obtained from the PC(I) data. It should be pointed out that all of the samples described above were also characterized by measuring the a.c. PC as a function of the modulation frequency; in all cases, the measurements were carried out at an intensity where linear carrier recombination was expected to dominate. By analysing the frequency dependence of the PC it was possible to extract the linear carrier lifetime, and in all cases the obtained value was near 10 μs. This value of the carrier lifetime was subsequently employed in all theoretical simulations [4].

2.2. Photothermal modulated optical reflectance behaviour

Experimental PMOR data were obtained under conditions for which the thermal component dominated the Drude component, using a variation of the apparatus described

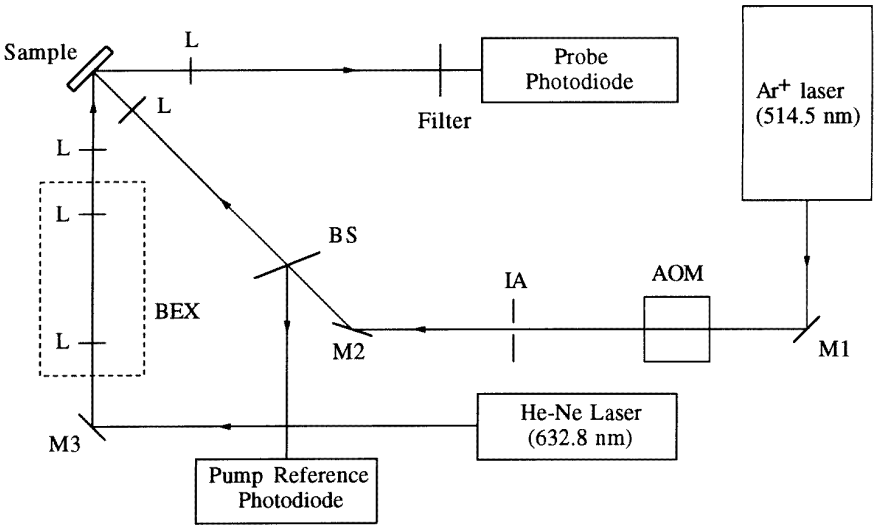

Figure 3. Schematic diagram of PMOR instrumentation: AOM, acousto-optic modulator; BEX, beam expander; BS, beamsplitter; IA, iris aperture; M, mirror; L, lens.

by Opsal *et al* [3]. Each sample described in table 1 was excited with a normally incident Gaussian beam of wavelength 514.5 nm (2.4 eV). Figure 3 shows the experimental set-up. The PMOR signal was measured as a function of absorbed pump power at two different modulation frequencies, 10 kHz and 1 MHz. At 10 kHz, the 1/e pump radius was 5.7 μm, and at 1 MHz two different pump radii were employed, 5.7 and 23.3 μm. The probe beam of wavelength 632.8 nm had an angle of incidence about 28°, and a Gaussian 1/e radius of 6.3 μm. Since the pump beam was rather tightly focused in order to improve the PMOR signal-to-noise ratio, the carrier and heat diffusion in the various samples had considerable three-dimensional character. In order to ascertain the dimensionality of the thermal diffusion problem for a given pump beam diameter φ, one must consider [3] the magnitude of the thermal diffusion length [1–3]. L_{T}, and the optical absorption length, L_α, as compared with φ. Specifically, thermal diffusion is 1D when $L_{\mathrm{T}}, L_\alpha \ll \varphi$. Likewise [3], carrier diffusion is 1D in nature when the carrier diffusion length [5], L_{D}, and L_α are much less than φ. Table 3 shows the various lengths discussed above for Si and Ge at 10 kHz and 1 MHz. Clearly, carrier diffusion was always 3D in nature in these experiments, while thermal diffusion had considerable 1D character, especially at 1 MHz.

Figure 4 shows the experimental PMOR amplitude ($\Delta R/R$) for the c-Ge sample as a function of the absorbed pump power (1/e radius = 5.7 μm, f = 10 kHz). Both theoretical modelling and experimental measurements for this sample indicate that the thermal component of the PMOR signal was much larger than the Drude component over all experimental conditions employed in the present study; thus, the PMOR amplitude for this sample should reflect the trends established for $T_2(0)$, the surface value of the a.c. temperature component [4]. In qualitative agreement with the theory, the c-Ge showed weakly supralinear behaviour as the pump power was increased; in particular, the signal made a transition from $I^{1.03}$ behaviour at low powers to $I^{1.16}$ behaviour at higher powers. The PC(I) data discussed in the previous section suggested that Auger recombination was dominant in the c-Ge at elevated pump powers; thus, based on [4], figure 6(a), one would expect the c-Ge PMOR amplitude to increase as $I^{1.06}$ at higher powers. The greater degree of supralinearity observed for the c-Ge experimentally may be due to the temperature dependence of the thermophysical properties of the semiconductor. The d.c. temperature increase of the illuminated spot with increased average pump-beam power is expected to have caused the thermal conductivity of the sample to decrease [9, 10]. This would lead the PMOR amplitude to increase above the value expected if the thermal conductivity were insensitive to temperature, as was assumed in the theory. With regard to the phase of the PMOR signal, the phase lag decreased slightly as the power was increased.

At 1 MHz, the c-Ge PMOR amplitude increased linearly with pump power but showed a certain degree of saturation at the highest powers (figure 5(a)). From figure 5(b), the PMOR phase lag displayed sizeable changes as the pump power was increased. From the foregoing discussion it is expected that the essentially totally thermal character of the PMOR signal should exhibit an increased phase lag with increasing incident power, owing to the effect of the temperature dependence of the thermal properties of the sample: the higher the temperature, the lower the conductivity/diffusivity of the crystal, resulting in an *increasing* thermal-wave phase lag, as shown in the case of a heating pump beam with 1/e radius of 23.3 μm. When the laser-beam size was decreased to 5.7 μm, however, the intense optical flux seems to have introduced a dominant nonlinear behaviour resulting in the phase of the signal *decreasing* with increased incident power, as predicted by the theoretical simulations of [4],

Table 3. Characteristic length scales used to determine the dimensionality of the heat and carrier diffusion equations for crystalline silicon and germanium.

Sample	L_T (μm) at 10 kHz	L_T (μm) at 1 MHz	L_D (μm)	L_α (μm)	φ (μm)
Si	54	5.4	100	0.017	12–48
Ge	34	3.4	100	0.68	12–48

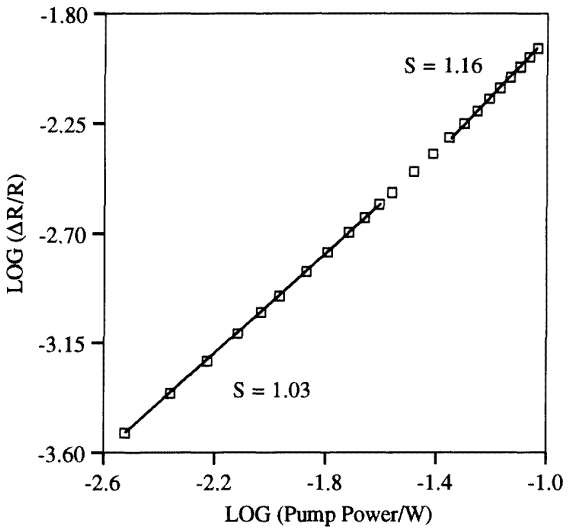

Figure 4. Normalized experimental PMOR amplitude ($\Delta R/R$) versus absorbed pump power for c-Ge. The 1/e pump radius is 5.7 μm and f = 10 kHz. The slopes of the linear sections are represented by the quantity S.

figure 6(*b*). Therefore, it follows that the phase variations of figure 5(*b*) were a combination of nonlinear effects such as nonlinear carrier recombination, and the dependence of the thermal conductivity on temperature. Since these large phase changes were accompanied by very slight saturation of the amplitude data, *it appears that the phase is more sensitive to nonlinear effects than is the amplitude.*

The c-Si1 material displayed stronger nonlinear PMOR behaviour than the c-Ge sample. Figure 6, curve (a), shows the PMOR amplitude versus the pump power at 10 kHz. The amplitude progressed from an $I^{1.07}$ to an $I^{1.48}$ dependence as the pump power was increased. Taking into account the clear indications of quadratic recombination in the PC(I) data discussed earlier, the high degree of PMOR supralinearity is not consistent with theory [4], and may be an indication of nonlinear surface effects. The phase lag, figure 6, curve (b), decreased progressively by about 3° over the same power range. It is also possible that 3D diffusion is at least partly responsible for the stronger than expected supralinear behaviour in the tight laser-beam spot-size geometry under which the PMOR data from the c-Si1 material were obtained. The c-Si1 PMOR amplitude at 1 MHz showed a weaker nonlinearity than was observed at 10 kHz ($< I^{1.20}$). Nevertheless, the 1 MHz phase lag changes were much larger than at 10 kHz (figure 7), with a greater tendency to decrease. *This indicates that the c-Si1 PMOR signal had a large Drude component at 1 MHz,* as

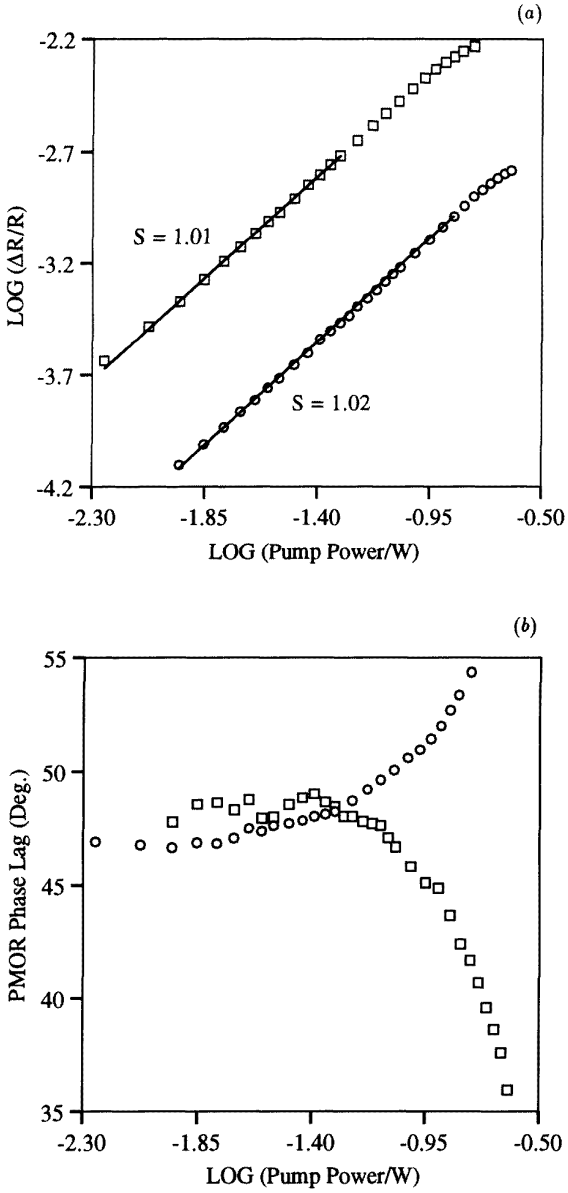

Figure 5. Normalized experimental PMOR amplitude ($\Delta R/R$) (*a*) and PMOR phase lag (*b*) versus absorbed pump power for c-Ge. The 1/e pump radius is (□) 5.7 or (○) 23.3 μm and f = 1 MHz. The slopes of the linear sections in (*a*) are represented by the quantity S.

shown in section 3.

At 10 kHz, the laser beam power dependence of the c-Si2 material behaved like the c-Ge sample. With regard to the PMOR amplitude (figure 8, curve (a)), a transition

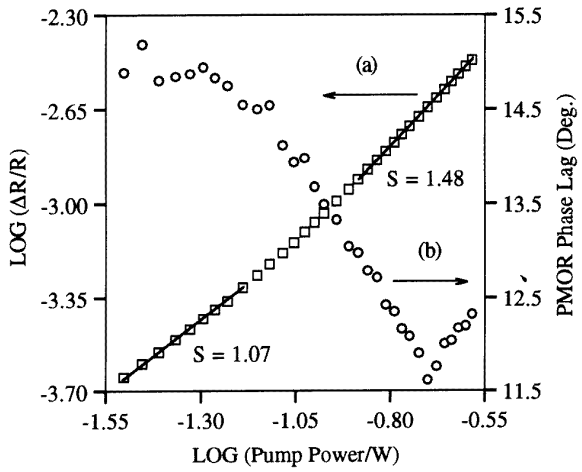

Figure 6. Normalized experimental PMOR amplitude ($\Delta R/R$) curve (a), and PMOR phase lag, curve (b), versus absorbed pump power for c-Si1. The 1/e pump radius is 5.7 μm and f = 10 kHz. The slopes of the linear sections in curve (a) are represented by the quantity S.

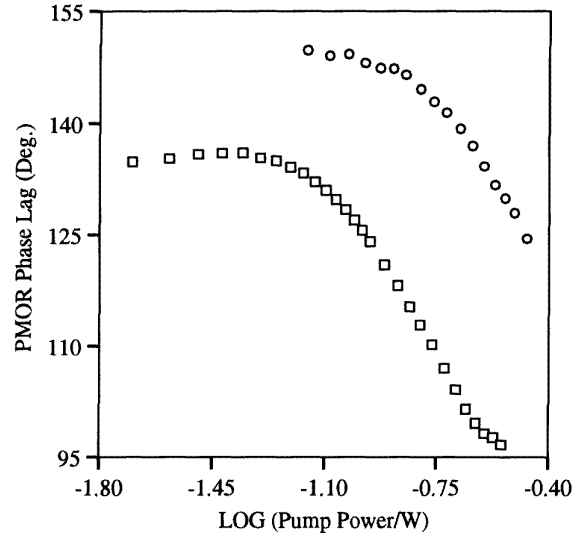

Figure 7. Normalized experimental PMOR phase lag versus absorbed pump power for c-Si1. The 1/e pump radius is 23.3 μm and f = 10 kHz (○) or 1 MHz (□).

from $I^{1.02}$ to $I^{1.10}$ behaviour was observed as the power was increased. This result is consistent with the evidence of Auger recombination provided by the PC(I) data of figure 2, curve (c). On the other hand, the increase in the phase lag with increasing power (figure 8, curve (b)) is indicative of a substantial contribution by the temperature dependence of the thermal conductivity, and not only of nonlinear carrier recombination. At 1 MHz, the c-Si2 PMOR amplitude was basically a linear function of the pump power, but there was some degree of saturation at the higher powers. The phase lag showed only small variations as the pump power was varied.

The c-Si3 sample, at 10 kHz, exhibited an extreme supralinear behaviour at low powers ($\propto I^{2.25}$), presumably

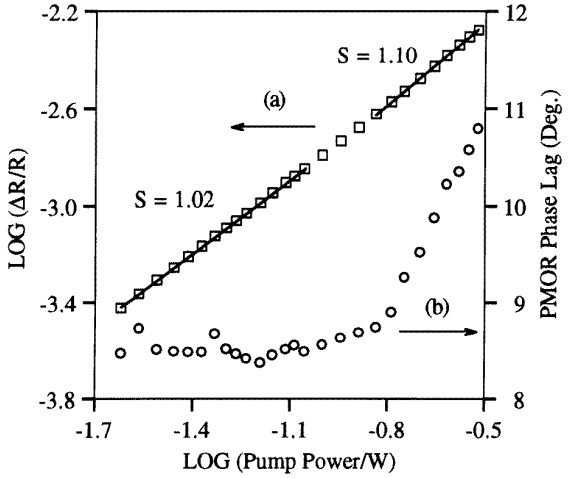

Figure 8. Normalized experimental PMOR amplitude ($\Delta R/R$), curve (a) and PMOR phase lag, curve (b), versus absorbed pump power for c-Si2. The 1/e pump radius is 5.7 μm and f = 10 kHz. The slopes of the linear sections in curve (a) are represented by the quantity S.

due to nonlinear surface recombination effects. This hypothesis is not surprising, considering that the PC(I) data of figure 2, curve (d), were also somewhat anomalous. This sample displayed quite a different PMOR behaviour at 1 MHz. With regard to the amplitude (figure 9(a)) with a laser beam radius of 23.3 μm, a transition from linear to strong sublinear behaviour with increasing power was observed, accompanied by a considerable decrease of the phase lag (figure 9(b)). Finally, the c-Si4 sample behaved very much like the c-Si3 material at 10 kHz, which points to a significant nonlinear surface effect. The data obtained at 1 MHz for the c-Si4 sample showed the same hybrid Drude/thermal effects seen for the c-Si3, and will be examined below. The fact that the c-Si3 and c-Si4 samples showed such similar PMOR behaviour, although they displayed quite different PC(I) trends, is in all likelihood the result of the enhanced sensitivity of the PMOR signal to the state of the semiconductor surface, compared to the PC signal.

3. Discussion: hybrid Drude and thermal behaviour

According to equation (1), the modulated reflectance is, in general, the superposition of two separate components, one proportional to the modulated carrier density (Drude effect) and the other proportional to the modulated temperature. When these two components are of a comparable size, and nonlinear carrier recombination is present, the intensity dependence of the PMOR signal may be quite irregular. In order to better understand some of the experimental PMOR data presented earlier, a simulation was carried out for c-Si assuming that the PMOR signal has hybrid Drude/thermal character. Equation (1) was utilized, taking into account the vectorial nature of ΔT and ΔN, to obtain ΔR.

The value of $\partial R/\partial T$ for silicon at 632.8 nm has been measured by Jellison and Burke [11], and is approximately

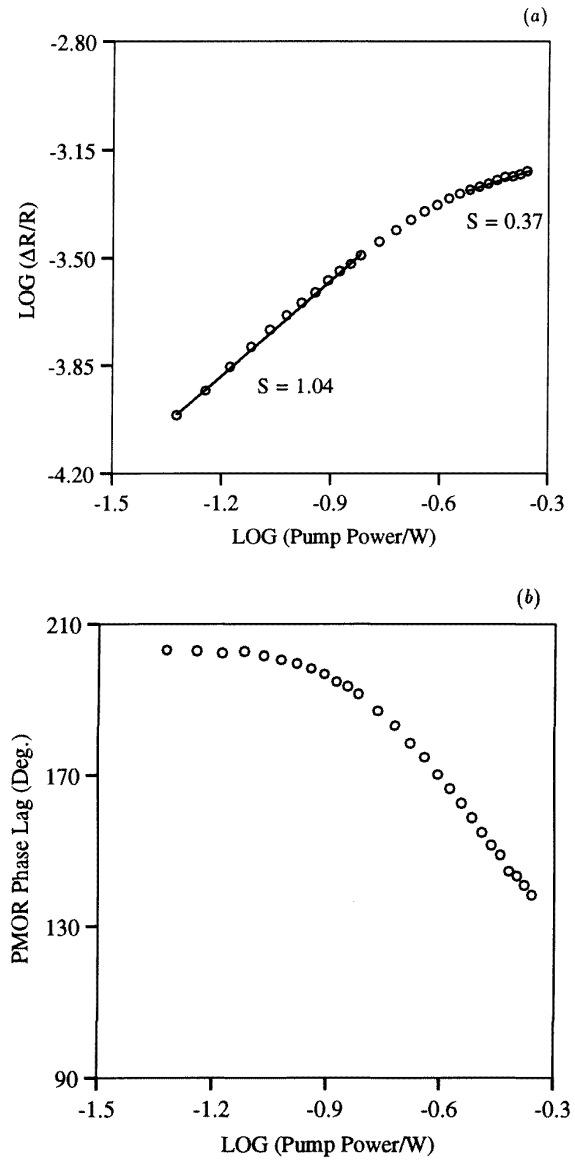

Figure 9. Normalized experimental PMOR amplitude ($\Delta R/R$) (*a*) and PMOR phase lag (*b*) versus absorbed pump power for c-Si3. The 1/e pump radius is 23.3 μm and f = 1 MHz. The slopes of the linear sections in (*a*) are represented by the quantity S.

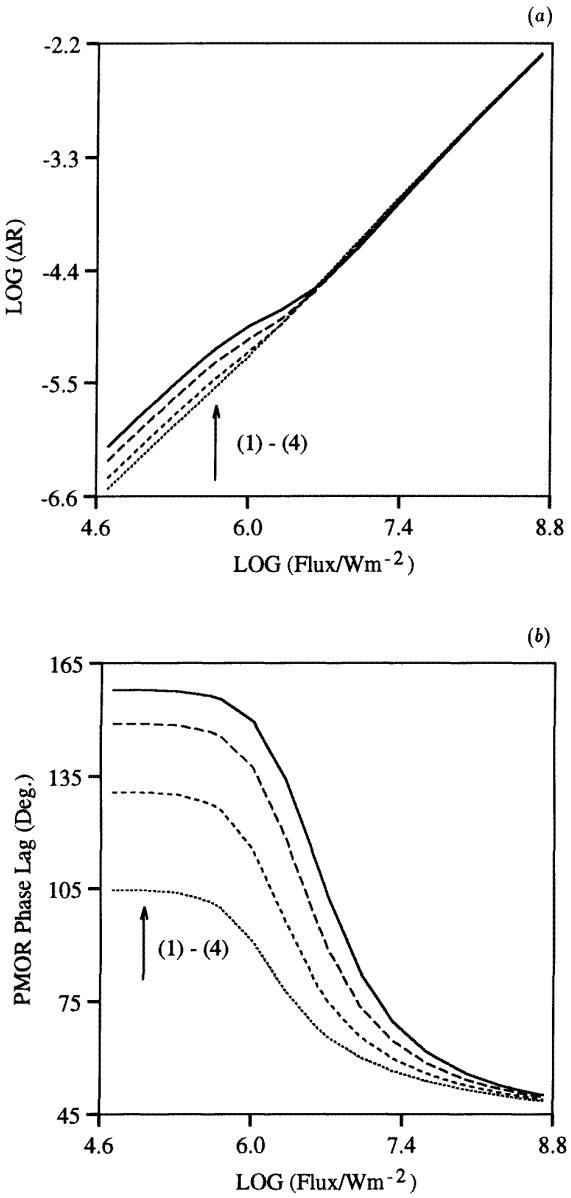

Figure 10. Theoretical simulation of ΔR amplitude (*a*) and phase lag (*b*) versus absorbed optical flux (W m^{-2}) for hybrid Drude/thermal PMOR signal. The sample is c-Si, both linear and Auger recombination are present, and the simulation parameters are given in the text (f = 10 kHz). The values of the Drude reflectance coefficient are: (1) -2.5×10^{-29}; (2) -4.0×10^{-29}; (3) -6.0×10^{-29}; (4) -8.0×10^{-29} m^3.

4.2×10^{-5} K^{-1}. Also, from Drude theory [12] and from the analysis of experimental PMOR data, the value of $\partial R/\partial N$ for silicon at 632.8 nm is expected to be in the range -2.5×10^{-29} to -8×10^{-29} m^3. Using simulation parameters which are typical for silicon [11] ($D = 3\times10^{-3}$ m^2 s^{-1}, $g_1 = 10^5$ s^{-1}, $g_3 = 4\times10^{-43}$ m^6 s^{-1}, $s_1 = s_2 = 0$, $\alpha = 10^6$ m^{-1}, $E_g = 1.1$ eV, $h\nu = 2.4$ eV, $\beta_s = 9.2 \times 10^{-5}$ m^2 s^{-1} and $k_s = 148$ W m^{-1} K^{-1}), the amplitude and phase lag of ΔR were calculated as a function of intensity, assuming the presence of linear and Auger recombination and solving equations (2) and (5) with the finite-difference technique [4]. Four different curves were obtained, with $\partial R/\partial N$ ranging from -2.5×10^{-29} to -8×10^{-29} m^3; the results are shown in figures 10(*a*) and 10(*b*).

For the PMOR amplitude curves of figure 10(*a*), considering the case where $\partial R/\partial N = -8 \times 10^{-29}$ m^3, at the lowest intensities ΔR is a linear function of I, and ΔR is dominated by the Drude component ($\propto \Delta N$). As the intensity rises, Auger recombination begins to overtake linear recombination, and ΔR shows a sublinear dependence on I. Eventually, the linearly increasing thermal component of ΔR dominates the Drude component, and ΔR increases in an approximately linear fashion again.

The simulated phase data depicted in figure 10(*b*) also clearly show the transition in the nature of the PMOR signal with increasing pump power, when nonlinear recombination is present. With $\partial R/\partial N = -8 \times 10^{-29}$ m^3, at the lowest intensities the phase lag has a constant value near 180°, which indicates that the Drude signal component is larger than the thermal component. As the intensity is raised the sublinear Drude component begins to be overtaken by the linear thermal component, and this is indicated by the decreasing phase lag in figure 10(*b*). At the highest intensities, the phase saturates at a value which indicates that the Drude signal component is much smaller than the thermal component. *Overall, if the phase lag changes by a large amount ($> 20°$) as the intensity rises, and $\partial R/\partial N < 0$ and $\partial R/\partial T > 0$, it ought to be concluded that the PMOR signal has a dual Drude/thermal nature, and that nonlinear carrier recombination is important.*

Based on the foregoing simulations, some of the experimental PMOR data presented in the previous section may be revisited for further qualitative interpretation. In the case of the c-Si1 phase data of figure 7 which could not be explained if only a thermal PMOR component was assumed to exist, the large phase changes are similar to those simulated in figure 10(*b*). Figure 7 clearly points to the existence of a hybrid Drude/thermal signal, and some type of nonlinear recombination effect. Nevertheless, the qualitative nature of the comparison of the data with the theory does not allow the complete clarification of the origin of the nonlinear effect; i.e. whether the large phase shifts observed in figure 7 should be attributed solely to the nonlinear *bulk* recombination simulated in figure 10(*b*), or whether a substantial component of nonlinear *surface* recombination should be added,

The c-Si3 material also showed evidence of dual Drude/thermal effects and nonlinear recombination. For the pump radius of 23.3 μm, figure 9(*a*), the sublinear amplitude curve at elevated intensities indicates that the Drude component was dominant at all powers, although the phase changes of figure 9(*b*) provide qualitative evidence that the thermal component was increasing in significance due to nonlinear recombination. The data obtained for the c-Si4 sample displayed similar patterns to those discussed for the c-Si3 sample, such as large phase variations pointing to dual Drude/thermal character, according to the trends in the simulation data of figure 10(*b*).

4. Conclusions

The nonlinear dependence of photothermal modulated reflectance (PMOR) and photocurrent (PC) signals on the laser pump beam intensity from a selection of Ge and Si wafers was studied. As expected from theoretical considerations [4], at high powers the samples all showed a sublinear intensity dependence, and the power-law exponents were successfully correlated with the theoretical results. The PC data were useful in this study because they clearly showed the presence of nonlinear recombination by directly probing the modulated carrier density; on the other hand, the PMOR signal tended to be dominated by thermal-wave effects, and carrier-wave domination could not be found even at the highest fluence levels, corresponding to laser beam radius of 5.7 μm.

Among the experimental PMOR data, two of the four silicon samples (c-Si3 and c-Si4) displayed very anomalous amplitude, $\Delta R/R(I)$, behaviour, and these results were assumed to be due to a nonlinear surface recombination velocity. Also, for these same samples the dependence of the phase lag on the excitation intensity was explained by noting that the PMOR signal is composed of two competing effects, namely the Drude and thermal components. When these two effects are of a similar magnitude, the PMOR amplitude and phase lag can show quite an irregular dependence on intensity. For two of the samples with a dominant thermal-wave signal component (c-Ge and c-Si2), the supralinear behaviour was basically consistent with the 1D simulations [4] for the modulated surface temperature. The slight departure from the model could be explained by invoking nonlinear thermal effects related to the temperature dependence of the sample thermal conductivity. The c-S1 material behaved somewhat anomalously at 10 kHz, and nonlinear surface recombination was invoked to explain its experimental behaviour; this sample also showed considerable hybrid Drude/thermal behaviour at 1 MHz.

Overall, this study concluded that when the PMOR signal has hybrid Drude/thermal character, nonlinear recombination may be clearly identified by large variations in the phase lag as the pump intensity is increased. The slope of the PMOR amplitude is also sensitive to nonlinear recombination, but not to the degree evidenced by the phase. Additional valuable information can be garnered for semiconductor samples (especially those with direct bandgaps) through the simultaneous monitoring of the radiative emission channel.

Acknowledgments

The authors wish to acknowledge partial support of this project by the Natural Sciences and Engineering Research Council of Canada through a Collaborative Research Grant.

References

[1] Smith W L, Rosencwaig A and Willenborg D L 1985 *Appl. Phys. Lett.* **47** 584
[2] Opsal J and Rosencwaig A 1985 *Appl. Phys. Lett.* **47** 498
[3] Opsal J, Taylor M W, Smith W L and Rosencwaig A 1987 *J. Appl. Phys.* **61** 240
[4] Wagner R E and Mandelis A 1996 *Semicond. Sci. Technol.* **11** 289
[5] Sze S M 1991 *Physics of Semiconductor Devices* 2nd edn (New York: Wiley) p 52
[6] Fournier D, Boccara C, Skumanich A and Amer N M 1986 *J. Appl. Phys.* **59** 787
[7] Dash W C and Newman R 1955 *Phys. Rev.* **99** 1151
[8] Philipp H R and Taft E A 1962 *Phys. Rev. Lett.* **8** 13
[9] Lietoila A, Gold R B, Gibbons J F and Christel L A 1984 *Semiconductors and Semimetals vol 17* ed R K Willardson and A C Beer (Orlando, FL: Academic) ch 2
[10] Meyer J R, Kruer M R and Bartoli F J 1980 *J. Appl. Phys.* **51** 5513
[11] Jellison G E Jr and Burke H H 1986 *J. Appl. Phys.* **60** 841
[12] Harrison W A 1979 *Solid State Theory* (New York: Dover) p 287